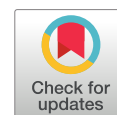## European Journal of Biology

Research Article   ⊙ **Open Access**

Identification of Karanjin's Molecular Targets for Colorectal Cancer Treatment Using Network Pharmacology and Molecular Docking

Khairah Ansari [1] ⬥ , Priyesh Kumar [1] ⬥ & Devendrasinh Jhala [1] ⬥ ✉

[1] Gujarat University, Biomedical Technology and Human Genetics University School of Sciences, Department of Zoology, Ahmedabad, Gujarat, India

Abstract

Objective: Colorectal cancer is a life-threatening condition. Karanjin, a furanoflavonol, has shown therapeutic potential against cancer. However, a comprehensive analysis of its mechanism of action is currently lacking. Hence, the primary objective of this study was to employ an integrated network pharmacology approach along with molecular docking to unravel the probable efficacy of karanjin in treating colorectal cancer.

Materials and Methods: Pharmacological assessments were performed using QikProp. Protein targets sourced from ChEMBL, Swiss target prediction, and PharmMapper were cross-referenced with colorectal cancer targets identified from GeneCards. A protein-protein interaction (PPI) network was generated using Cytoscape. Key targets were identified using cytoHubba. Functional insights were obtained through GO and KEGG analyses using DAVID. A Compound–Disease–Pathways–Targets Network was developed based on integrated data. Molecular docking was performed using YASARA. Finally, to validate the stability of the docked ligand-protein complexes, MD simulations were conducted.

Results: Karanjin met the ADME criteria and exhibited interactions with 270 targets, including 263 individuals linked to diseases. The topological analysis of the PPI network identified 24 targets. GO analysis yielded 20 terms, mainly associated with signal transduction, protein binding, and the cytosol. KEGG analysis identified 20 signalling pathways, with pathways in cancer being the most prominent. Using these data, Compound-Disease-Pathways-Targets network was constructed. Molecular docking and simulations highlighted strong interactions between AKT1 and HSP90AA1.

Conclusion: This study indicated that karanjin may exhibit anticancer properties against colorectal cancer via modulating PI3K-Akt signalling pathway. This study provides a building block for further research.

Keywords Karanjin · Network Pharmacology · Molecular Docking · Molecular Simulation

INTRODUCTION

In a society experiencing rapid development and improving standards of living, cancer is regarded as an ever-growing threat. Cancer develops from the transformation of normal cells into tumour cells as they progress from precancerous lesions to malignant tumours over the course of many stages.[1] Cancer rates for colon cancer rank third among all cancers worldwide, with an expected incidence rate of 2.4 lakhs by 2035.[2] Significant technological advances have been achieved primarily in conventional therapies, but cancer remains a leading cause of mortality for several reasons.

For the treatment of cancer, targeting or suppressing a single gene product or specific signalling pathway, which may have up to 500 distinct dysregulated genes, is unlikely to be effective in treating cancer.[3,4] The majority of cancer treatment development is still focused on modulating individual targets, usually one at a time, with compounds dubbed "targeted therapies," "smart drugs," or "magic bullets." To increase efficiency of cancer treatment, the current paradigm of chemotherapy is a combination of multiple drugs and radiation therapy, each with a particular mode of action.[5] The Food and Drug Administration (FDA) has approved several drugs that modify multiple targets. However, these medications are expensive, have an extensive list of unfavourable side effects, and are ineffective in changing the course of the disease. Investigating the plant kingdom may yield promising directions for the swift advancement of new anticancer agents. Numerous phytochemicals are increasingly recognised as a valuable source of effective yet safer treatments for various types of cancer.[6] However, the molecular targets of these natural compounds and their true potential as anticancer agents remain unknown.

With advances in computer technology, network pharmacology has emerged, combining various fields to study drug actions and interactions with multiple targets.[7] Network pharmacology is now extensively utilised to explore the molecular mechanisms underlying drug actions, providing deeper insights into how drug-like substances work at the cellular and molecular levels.[8] Molecular docking is a widely recognised structure-based computational technique in drug discovery that predicts ligand-target interactions, aiding in the identification of new medicinal compounds. Recent studies have also explored combining docking with molecular dynamics (MD) to improve the accuracy of virtual screening predictions.[9]

Karanjin is a principal furanoflavonol constituent present in the seeds of the medicinal plant *Millettia pinnata*. Earlier reports have confirmed the voluminous action of karanjin as an anticancer agent in cell lines A549, HepG2, HL-60 and HeLa.[10,11] Karanjin also induced apoptosis in dimethylhydrazine-induced colon carcinoma in rats by downregulating the anti-apoptotic proteins Bcl2 and p53, whereas it upregulated the expression of BAX.[12] However, the detailed molecular mechanism of karanjin in treating colorectal cancer is still unclear. The present study aimed to investigate the potential inhibitory effects of the drug using a network pharmacology approach. The initial steps involved collecting the potential targets of karanjin and the targets associated with colon cancer. Subsequently, common genes were identified and used to construct Protein-Protein Interaction (PPI) and Compound- Disease -Pathways- Targets networks. The Gene Ontology (GO) and Kyoto Encyclopedia of Genes and Genomes (KEGG) analysis were performed. Finally, molecular docking and simulation were used to validate the action of karanjin with its core targets.

MATERIALS AND METHODS

Screening Chemical Structures from the PubChem Database

The chemical structure of karanjin (PubChem CID: 100633) was obtained from the PubChem Database (https://pubchem.ncbi.nlm.nih.gov/). PubChem is an open chemistry database, and it is the largest and freely accessible online server.

Analysis of the Pharmacokinetic Properties of Karanjin

The drug-like properties of karanjin were assessed by predicting the absorption, distribution, metabolism, and excretion of ADME (Figure 1). QikProp 4.4 (Schrödinger, LLC, New York) was used to analyse these properties. The canonical SMILES of karanjin was retrieved from the PubChem database. The force field was set to OPLS 2005, and all other parameters were kept constant. QikProp estimates a wide range of pharmaceutically relevant properties. Karanjin was also analysed to be consistent with Lipinski's rule of five, which should be considered for the development of a successful drug.[13]

Identification of Potential Protein Targets

The potential protein target of karanjin was predicted using web tools viz., Swiss Target Prediction (http://www.swisstargetprediction.ch/), ChEMBL (https://www.ebi.ac.uk/chembl/), and PharmMapper (https://www.lilab-ecust.cn/pharmmapper/) tools. Swiss Target Prediction is a freely available web service that is used to identify the targets of small bioactive molecules in vertebrates, including humans. Swiss Target Prediction is also applicable to determining
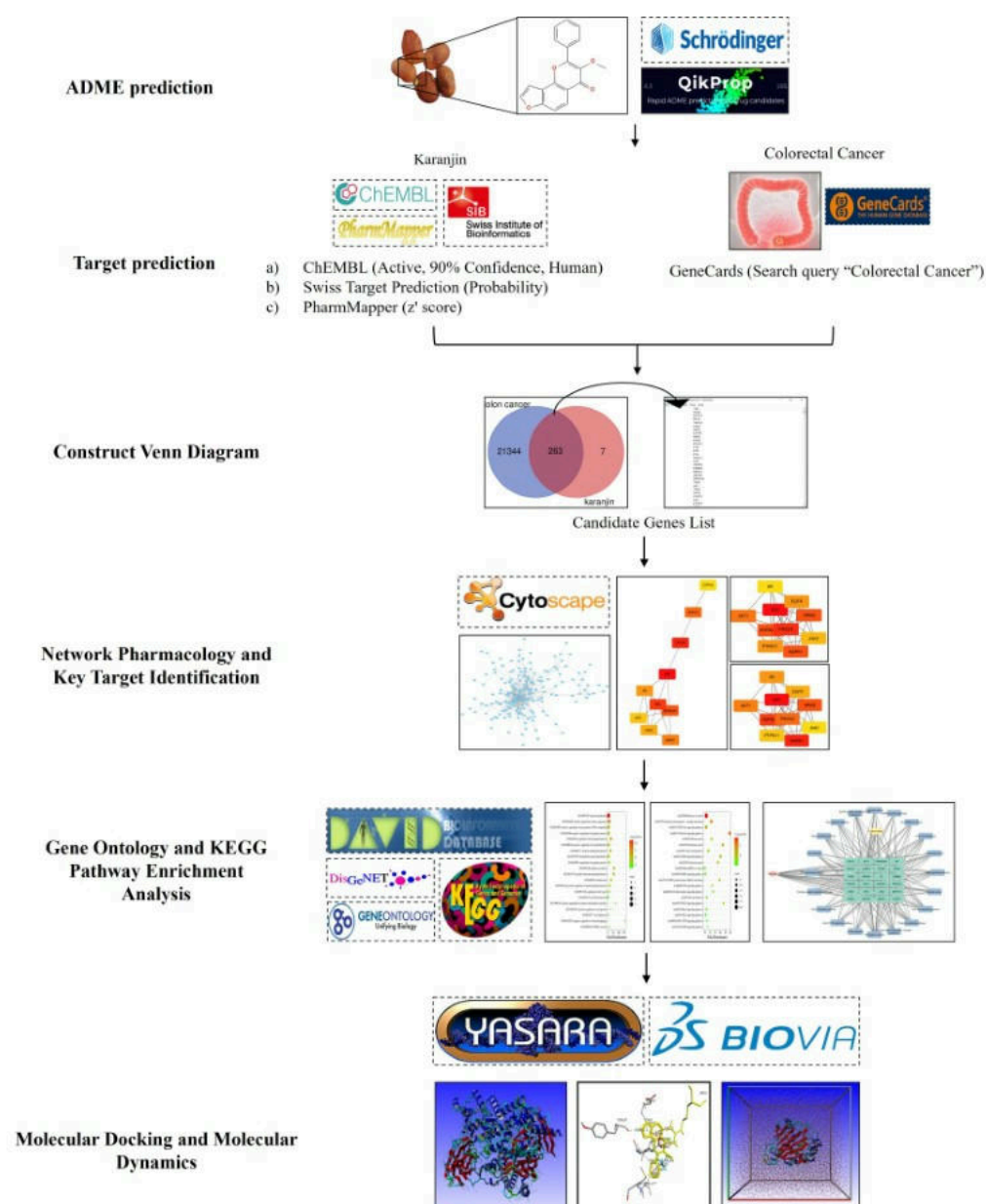
Figure 1. Flowchart of the work.

the macromolecular targets of a small molecule that is considered bioactive.[14] The canonical SMILES of karanjin was used to predict targets using Swiss Target Prediction. The term "karanjin" was used to search targets in ChEMBL. ChEMBL is an open data repository that includes interaction, functional, and ADMET data for a wide range of bioactive compounds that possess drug like properties.[15] The 2D structure of karanjin in sdf format was used to identify targets using PharmMapper.

Acquisition of Known Targets of Colorectal Cancer

The target genes related to the pathogenesis of colorectal cancer were identified using GeneCards (www.genecards.org). The colorectal cancer and karanjin associated protein targets were then imported into the Venn diagram (https://bioinformatics.psb.ugent.be/webtools/Venn/).

The intersection genes were retrieved to identify candidate genes.

PPI Network Analysis

Using STRING in Cytoscape (version 3.9.1 software (https://cytoscape.org/), a PPI network of candidate genes was created with a confidence level of 0.9. Cytoscape is an open-source software that is used for integrating, visualising, and analysing biological networks.[16] The key targets were assessed based on the topological features of "degree," "betweenness," and "closeness" (Figure 1).

GO and KEGG Enrichment Analyses

GO and KEGG enrichment analysis was performed using the Database for Annotation Visualisation and Integrated

Discovery DAVID (https://david.ncifcrf.gov/). The key target list in the form of a gene identifier was uploaded in the DAVID input box. The list was submitted to start the analysis. The DAVID database facilitates the functional annotation and analysis of a large number of genes.[17] GO functionally categorises key genes into three main categories: cellular components (CCs), molecular functions (MFs), and biological processes (BPs). At the molecular level, the functional implications can be assigned to genes using GO. KEGG enrichment analysis revealed potential biological pathways involving key genes.[18] The SR plot (https://www.bioinformatics.com.cn/en) of the shortlisted key target list was used to generate a bubble chart for enrichment analysis (Figure 1).

Construction of Compound-Disease-Pathways-Targets Network

A network of Compound-Disease-Pathways-Targets (CDPT) was created to reveal the pharmacotherapeutic mechanism of karanjin. The DAVID database was used to obtain the DisGeNET data. The data from KEGG pathway and PPI network were obtained using cytoscape software. Further, using the "merge" tool of cytoscape software version 3.9.0, all networks were merged to form the final network. In the network nodes for drug and disease, target genes, and disease-related pathways were represented with different colours and shapes using the yFiles layout algorithm of the cytoscape tool.

Acquisition of Protein Structure

The 3D crystal structures of six different target proteins scrutinised by topological parameter i.e. SRC (2bdf), AKT1 (3o96), MAPK1 (1tvo), HRAS (5p21), HSP90AA1 (4nh8), and PIK3CA (2rd0), were obtained from the RCSB Protein Data Bank (RCSB PDB) (https://www.rcsb.org/). Established in 1971, the Protein Data Bank (PDB) was the first publicly accessible digital library in the biological sciences. The active site of the protein was determined using the Computed Atlas of Surface Topography of Proteins (CASTp) (http://sts.bioe.uic.edu).[19]

Molecular Docking

Molecular docking was performed using the YASARA 22.5.22 software. The molecular docking methodology examines the behaviour of small molecules in a target protein's binding site. The proposed method is based on the AutoDock Vina platform.[20] The proteins and ligands were prepared using YASARA. During protein and ligand preparation, water molecules were removed, hydrogen atoms were added, and energy was minimised, while a simulation cell was also defined around the active site of the protein. The macrofile

dock_run.mcr was used to calculate the interaction energy between the protein receptor and karanjin. The higher the docking score in YASARA, the better the protein-ligand interaction, whereas a negative value indicates no binding. After docking, the docked complexes were visualised and converted into PDB files. The protein-ligand interactions were further visualised in 3D and 2D using the Discovery Studio visualiser (Figure 1).

Molecular Dynamics (MD) Simulation

MD simulations of the docked ligand-receptor complexes AKT1-karanjin and HSP90AA1-karanjin was conducted using YASARA version 22.5.22 based on high binding energy. The simulation ran for 100 ns with the AMBER 14 force field. A cubic simulation cell was created with dimensions of 100.04 Å x 100.04 Å x 100.04 Å. Energy minimisation was performed using the steepest gradient method to alleviate any steric clashes. The pH and physiological temperature were maintained at 7.4 and 298 K, respectively. To mimic a physiological saline environment, water molecules and NaCl counter-ions (0.15 M) were added to the simulation cell. The macrofile md_run.mcr facilitated the simulation, which was performed over 100 ns with trajectory files generated every 100 ps to record the dynamics of interactions. After the simulation, the resulting files were analysed using md_analyze.mcr and exported in .tab format for graphical representation.

RESULTS

Pharmacokinetic Analysis

The drug like properties of karanjin were assessed using QikProp. The results (Table 1) show that karanjin exhibits high human oral absorption at 100% and QPP Caco-2 of 3979.043 nm/s. Other pharmacokinetic parameters, such as QPlogPo/w=3.33, QPlogS of –3.564 mol dm⁻³, QPlogKhsa=0.104, and PSA=51.639, were all within the acceptable range for human use.

Candidate Genes Associated with Karanjin and Colorectal Cancer

A total of 168 target genes based on a high z' score from PharmMapper were selected. The z' score is derived from the fit score of the molecule and a library score matrix. PharmMapper identifies the optimum mapping poses of the query molecule against all pharmacophore models.[21] The target prediction through the ChEMBL database gives "active" or "inactive," depending on whether karanjin is projected to interact with the target or not. From the ChEMBL database, 13 active targets with a confidence level of 90% were selected. The targets are predicted by reverse screening based on the

**Table 1.** Pharmacokinetic properties: absorption, distribution, metabolism, and excretion (ADME) of karanjin.

Sr. No.	Property/Descriptor	Karanjin	Permissible Limit
1	#stars[a]	0	0-5
2	CNS[b]	1	–2 (inactive), +2 (active)
3	mol_MW;[c]	292.29	130.0 – 725.0
4	QPlogPo/w[d]	3.33	–2.0-6.5
5	QPlogS[e]	–3.564	–6.5 -0.5
6	QPlogHERG[f]	–5.303	concern below –5
7	QPPCaco[g]	3979.043	<25 poor, >500 great
8	QPlogKhsa[h]	0.104	–1.5 – 1.5
9	HumanOralAbsorption[i]	3	1, 2, or 3 for low, medium, or high
10	PercentHumanOral Absorption[j]	100	>80% is high <25% is poor
11	PSA[k]	51.639	7.0 – 200.0
12	RuleOfFive[l]	0	maximum is 4
13	RuleOfThree[m]	0	maximum is 3

[a]Number of propertyor descriptor values that fall outside the 95% range of similar values for known drugs. [b] Predicted central nervous system activity on a –2 (inactive) to +2 (active) scale. [c] Molecular weight of the molecule. [d] Predicted octanol/water partition coefficient. [e] Predicted aqueous solubility, log S. S in mol dm^{-3} is the concentration of the solute in a saturated solution that is in equilibrium with the crystalline solid. [f] Predicted IC$_{50}$ value for blockage of HERG K$^+$ channels. [g] Predicted apparent Caco-2 cell permeability in nm/s. Caco2 cells are a model for the gut-blood barrier. [h] Prediction of binding to human serum albumin. [i] Predicted qualitative human oral absorption: 1, 2, or 3 for low, medium, or high. [j] Predicted percent human oral absorption on a 0 to 100% scale. The prediction is based on a quantitative multiple linear regression model. [k] Van der Waals surface area of polar nitrogen and oxygen atoms. [l] Number of violations of Lipinski's rule of five. [m] Number of violations of Jorgensen's rule of three.

similarity principle in Swiss Target Predictions.[14] A total of 100 target genes with high probability were acquired from the Swiss Target Predictions. After eliminating duplicates, 270 genes were recognised as potential targets of karanjin. From GeneCards, 21.607 known targets for colorectal cancer were identified. Ultimately, 263 intersecting genes were selected as candidate genes for further investigation (Figure 2).

PPI Network Analysis

A PPI network was built based on the 263 candidate genes by importing them into the cytoscape, with the highest confidence level of 0.9. The PPI network comprised 176 nodes and 542 edges (Figure 3A). Additionally, two primary protein-protein interaction clusters were identified using the MCODE algorithm. The first cluster (Figure 3B) included 19 nodes and 39 edges, featuring core genes such as HRAS, MAPK1, MAPK8, and STAT1. The second cluster (Figure 3C) comprises
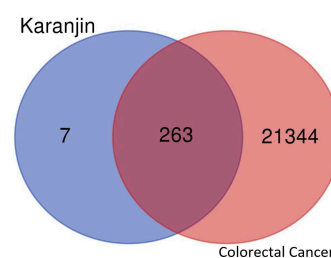
Figure 2. A Venn diagram illustrates the overlap between 263 candidate genes identified as potential targets of the compound karanjin and 21,607 known targets for colorectal cancer.

Table 2. The topological parameters, viz. degree, betweenness, and closeness centrality, were determined using the cytohubba tool of cytoscape software for the major targets of karanjin for colorectal cancer.

Sr. No.	GeneID	Degree	Betweenness	Closeness
1	SRC	41	5542.887	94.067
2	AKT1	30	3855.929	88.126
3	MAPK1	30	2773.450	88.443
4	HRAS	30	2640.921	86.876
5	HSP90AA1	28	3290.569	86.800
6	PIK3CA	28	1299.068	83.302
7	RXRA	22	3765.790	80.683
8	ESR1	19	1212.546	80.050
9	AR	19	1707.364	82.017
10	MAPK14	18	840.192	78.502
11	NR3C1	18	1037.992	79.476
12	JAK2	18	328.393	77.893
13	MAPK8	17	2063.028	78.402
14	HDAC1	16	836.641	73.043
15	F2	14	2186.691	73.819
16	STAT1	14	338.134	75.633
17	PRKACA	13	1601.875	72.460
18	CASP3	13	1231.867	71.944
19	CDK4	13	795.684	75.143
20	MAP2K1	13	354.165	73.702
21	ERBB4	12	102.712	71.593
22	PIK3CB	12	69.325	72.319
23	MTOR	10	551.901	70.293
24	CDK6	10	318.30217	70.47619

7 nodes and 17 edges. In the analysis of the initial network using various algorithms, only nodes with elevated values of "degree," "betweenness," and "closeness" were considered key targets. Finally, 24 key targets were collected for pathway enrichment analysis, with the top three being AKT1, MAPK1, and SRC (Table 2).

GO Enrichment Analysis

The gene list was submitted to the DAVID web tool to functionally annotate the impact of key targets in BPs, CCs, and MFs. As shown in Figure 4A, Figure 4B, and Figure 4C, enriched BPs, CCs, and MFs (p<0.01) term includes signal transduction GO:0007165, protein binding GO:0005515, and cytosol GO:0005829, respectively. The dot size indicates the quantity of targets linked to a particular term, while the colour represents the log10 (p-value). The enrichment along the x-axis represents the ratio of target genes associated with all annotated genes within the pathway.

The CC annotations (Figure 4B) analysis identified several cellular components, including the nucleoplasm GO:0005654, cytoplasm GO:0005737, and nucleus GO:0005634, which were targeted by karanjin. According to GO, MFs (Figure 4C) the major activities associated with the targets are ATP binding GO:0005524 and protein serine/threonine/tyrosine kinase activity GO:0004712. Further BP terms (Figure 4A) showed that

key genes were involved in the positive regulation of cell proliferation GO:0008284, negative regulation of apoptotic process GO:0043066, cell migration GO: 0016477, MAPK cascade GO:0000165. BP enrichment showed that identified target genes were significantly associated with cancer cell survival, proliferation, migration, and differentiation.

KEGG Enrichment Analysis

KEGG enrichment analysis was conducted to identify the pathways linked to important targets, resulting in the identification of 20 significant signalling pathways with significance level p<0.01. The dot size indicates the quantity of targets linked to a particular term, while the colour represents the log10 (p-value). The enrichment along the x-axis represents the ratio of target genes associated with all annotated genes within the pathway (Figure 4D). The pathways in cancer (hsa05200) were recognised as the most important with the highest amount of target enrichments and lowest p value. The PI3K-Akt signalling pathway (hsa04151), MAPK
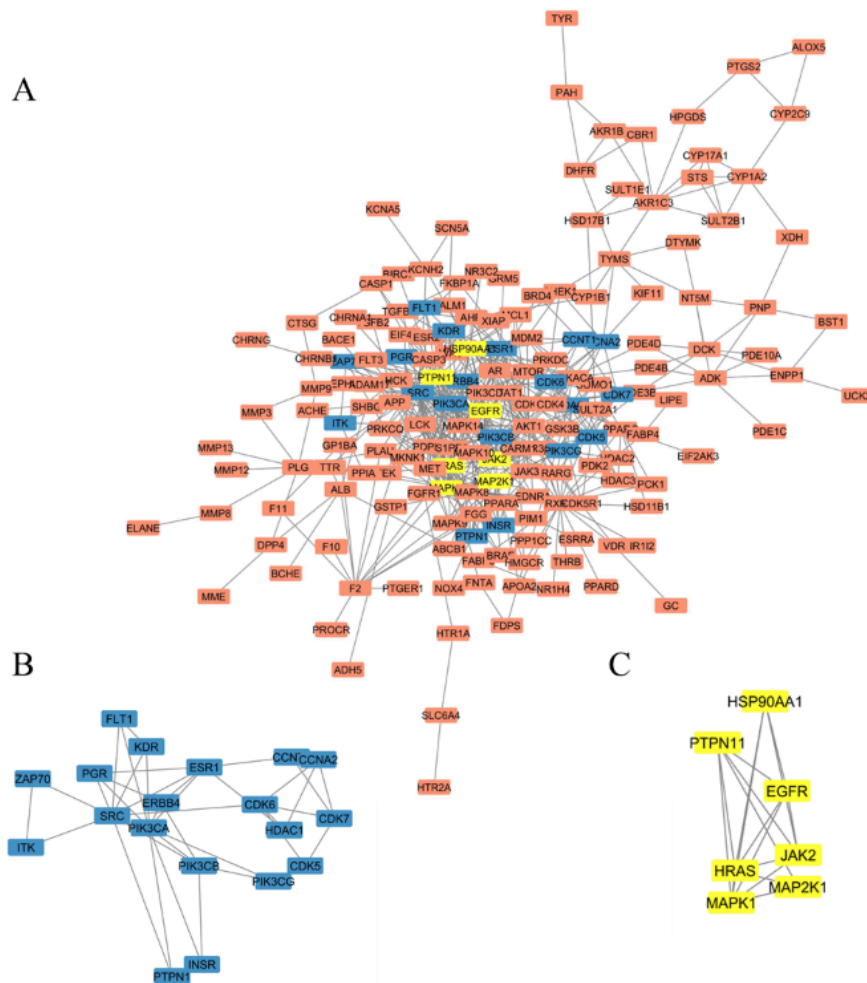

Figure 3. (A) PPI (Protein-Protein Interaction) Network of all candidate gene targets of karanjin with 176 nodes and 542 edges at a confidence level of 0.9; (B) A protein-protein cluster with 19 nodes and 39 edges was identified using the Molecular Complex Detection (MCODE) algorithm; (C) A smaller MCODE cluster was identified with 7 nodes and 17 edges.

signalling pathway (hsa04010), Colorectal cancer (hsa05210), mTOR signalling pathway (hsa04150) (Figure 4D).

Compound-Disease-Pathways-Targets (C-D-P-T) Network

Recent advances in genomics have prompted a paradigm shift in drug discovery from an emphasis on strong single-target interactions towards a more global and comparative investigation of multitarget networks. The (C-D-P-T) network (1 compound, 24 targets, 20 pathways and 1 disease) is shown in Figure 5. Following that, 6 main targets for karanjin were identified using the CDPT network (Figure 5), the majority of which were involved in each pathway in the pathogenesis of colon cancer.

Molecular Docking

For molecular docking with karanjin, a total of 6 target genes with strong interactions with other targets, pathways, and potential components were selected. The proteins included SRC (2bdf), AKT1 (3o96), HSP90AA1 (4nh8), HRAS (5p21), MAPK1 (1tvo), and PIK3CA (2rd0). These proteins are involved in the pathogenesis of colorectal cancer. A higher binding energy indicates more favourable protein-ligand interaction. According to the molecular docking results presented in Table 3, karanjin has the highest binding energy with AKT1, i.e., 10.54 kcal/mol. The findings indicated that karanjin demonstrates stronger interactions with AKT1 (10.54 kcal/mol), HSP90AA1 (9.35 kcal/mol), HRAS (9.14 kcal/mol), and MAPK1 (8.57 kcal/mol) compared with their respective positive inhibitors, Idelalisib (9.53 kcal/mol),
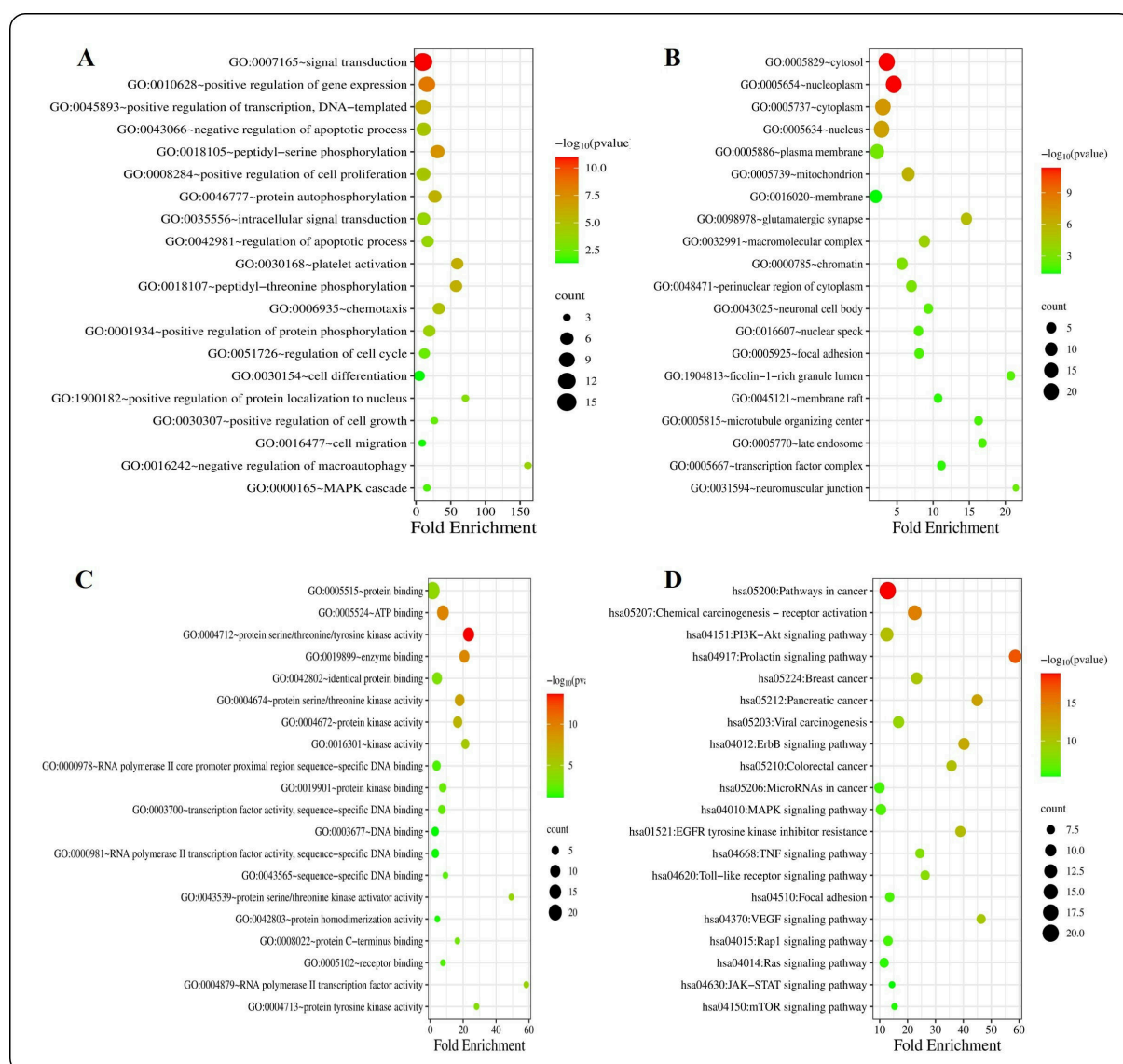

Figure 4. Bubble plot generated using SR plot (A) GO Biological processes; (B) GO Cellular Components; (C) GO Molecular Functions; (D) KEGG enrichment. The size and the colour of the dot reflect the number of target genes and -log10 (p-value) respectively associated with these terms.

Irsogladine (8.60 kcal/mol), Tipifarnib (7.90 kcal/mol), and FR180204 (8.03 kcal/mol). For SRC, the positive inhibitor, Dasatinib, exhibited stronger binding affinity (8.49 kcal/mol) than karanjin (7.82 kcal/mol). Similarly, the positive inhibitor of PIK3CA, Alpelisib, showed a higher binding affinity (9.33 kcal/mol) than karanjin (7.93 kcal/mol). Figure 6 illustrates that karanjin interacts strongly with the key binding pocket of the protein. This interaction involves multiple binding modes, including hydrogen bonding, carbon hydrogen bonding, Pi-alkyl/Pi-Pi stacked/Pi-Cation/Pi sigma/Pi-Pi T-shaped interactions within the active site.

MD Simulation

Based on the docking results, the AKT1 and HSP90AA1 protein-ligand complexes were selected for the 100-ns MD simulation. In this study, two protein-karanjin complexes were subjected to MD simulation by root-mean-square deviation (RMSD), root-mean-square fluctuation (RMSF), and radius of gyration (Rg) analysis.

The RMSD analysis assessed the stability and conformational changes of AKT1 and HSP90AA1, with lower molecular deviations indicating higher protein stability. According to the RMSD analysis, the RMSD values of HSP90AA1 protein
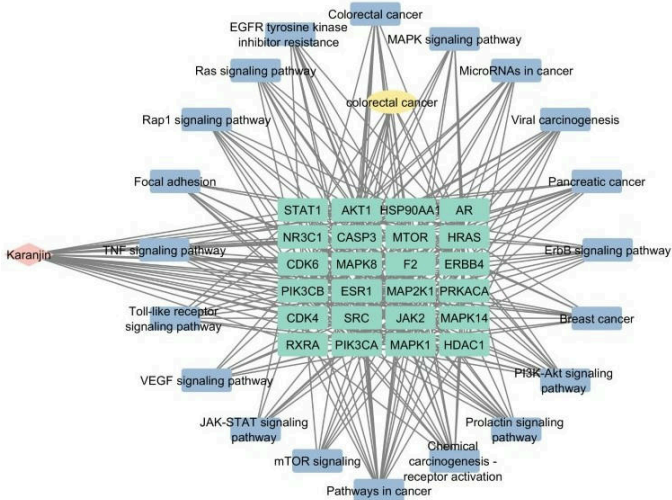

Figure 5. The compound-disease pathways target network was constructed with 46 nodes and 326 edges using the STRING plugin in Cytoscape software. This network visually illustrates the complex connections among karanjin, colorectal cancer, associated pathways, and key targets. The pink diamond-shaped node represents karanjin; yellow node represents disease colorectal cancer acquired from the DisGeNet database from the DAVID web tool; purple and green rectangular nodes represent pathways acquired from the KEGG database from the DAVID web tool and key targets acquired using the cytohubba tool from cytoscape.

Table 3. Molecular docking results comparing the binding affinities of selected proteins with those of karanjin and FDA-approved drugs.

Sr. No.	Target (PDB ID)	Binding energy (Kcal/mol)	Karanjin					
		Positive Inhibitor	Karanjin	Hydrogen bond (HB) interactions	HB (Å)	Pi-alkyl/Pi-Pi stacked/Pi-Cation/Pisigma/Pi-Pi Tshaped, Pi-Sulphur	Van der Waals interactions	Carbon hydrogen bonds
1	SRC (2bdf)	8.49	7.82	-	-	VAL281, ALA293, LYS295, LEU393, and LEU273	GLN275, GLY274, GLY276, SER345, ASP348, MET341, GLU339, TYR340, THR338, VAL323, ASP404	GLY344
2	HSP90AA1 (4nh8)	8.6	9.35	TRP162	2.80671	LEU107, PHE138, TYR139, VAL150, and MET98	ASP54, LYS58, ALA55, THR184, VAL186, LEU103, GLY108, VAL136, GLY135	-
3	PIK3CA (2rd0)	9.33	7.93	GLU596	2.27362	LYS594, LYS627, MET599, LEU623,PRO595, ILE823, ILE819	ASN822, LEU997, ASN826, and TYR622	GLN630
4	AKT1 (3o96)	9.53	10.54	SER205	2.92688	TYR272, TRP80, GLN79, LEU210, LEU264, and VAL270	ASN54, ILE290, THR291, THR211, LEU213, ALA212	LYS268, SER205
5	HRAS (5p21)	7.9	9.14	LYS117, ASP33	2.52967, 2.155405	LYS147, ALA18, PHE28, ALA146, and LYS117	VAL14, GLY15, VAL29, SER17, GLU31, TYR32, GLY13, ASP30, LEU120, ASN116, ASP119, SER145	-
6	MAPK1 (1tvo)	8.03	8.57	LYS54	2.86936	VAL39, LEU156, and ALA52	GLU71, ILE53, VAL104, GLN105, CYS166, ASP167, ARG67, TYR36, GLY37, ASN154, SER153, ILE103	-

(Figure 7A) during interaction with karanjin range between 0.385 Å and 1.567 Å with a mean value of 1.185 Å. The mean RMSD value of AKT1 protein (Figure 8A) during interaction with karanjin obtained was 1.491 Å with a minimum value of 0.419 Å and a maximum value of 2.091. The karanjin-HSP90AA1 complex was shown to be stable throughout the 100-ns simulation period, with just a minor fluctuation between 20 and 25 ns that was within acceptable limits. The karanjin-AKT1 complex was stable throughout the 100-ns simulation. Karanjin-HSP90AA1 showed lower deviation and fluctuation than the karanjin-AKT1 complex. Throughout the 100-ns simulation with HSP90AA1 and AKT1, the average RMSD

value for karanjin was 2.544 Å and 5.963 Å respectively. The RMSD values of karanjin with HSP90AA1 (Figure 7B) and AKT1 (Figure 8B) ranged from 0.52 Å to 5.93 Å and 0.751 Å to 7.951 Å respectively. The RMSD results indicated that karanjin was more stable with HSP90AA1 than with AKT1.

Figure 7C shows the Rg analysis of the karanjin-HSP90AA1 complex. According to the Rg analysis, the Rg ranged from 16.771 Å to 17.305 Å with a mean value of 17.048 Å. Figure 8C shows the Rg analysis of the karanjin-AKT1 complex. The mean Rg value of karanjin-AKT1 obtained was 20.102 Å with the lowest value of 19.663 Å and the highest value of 20.359 Å.
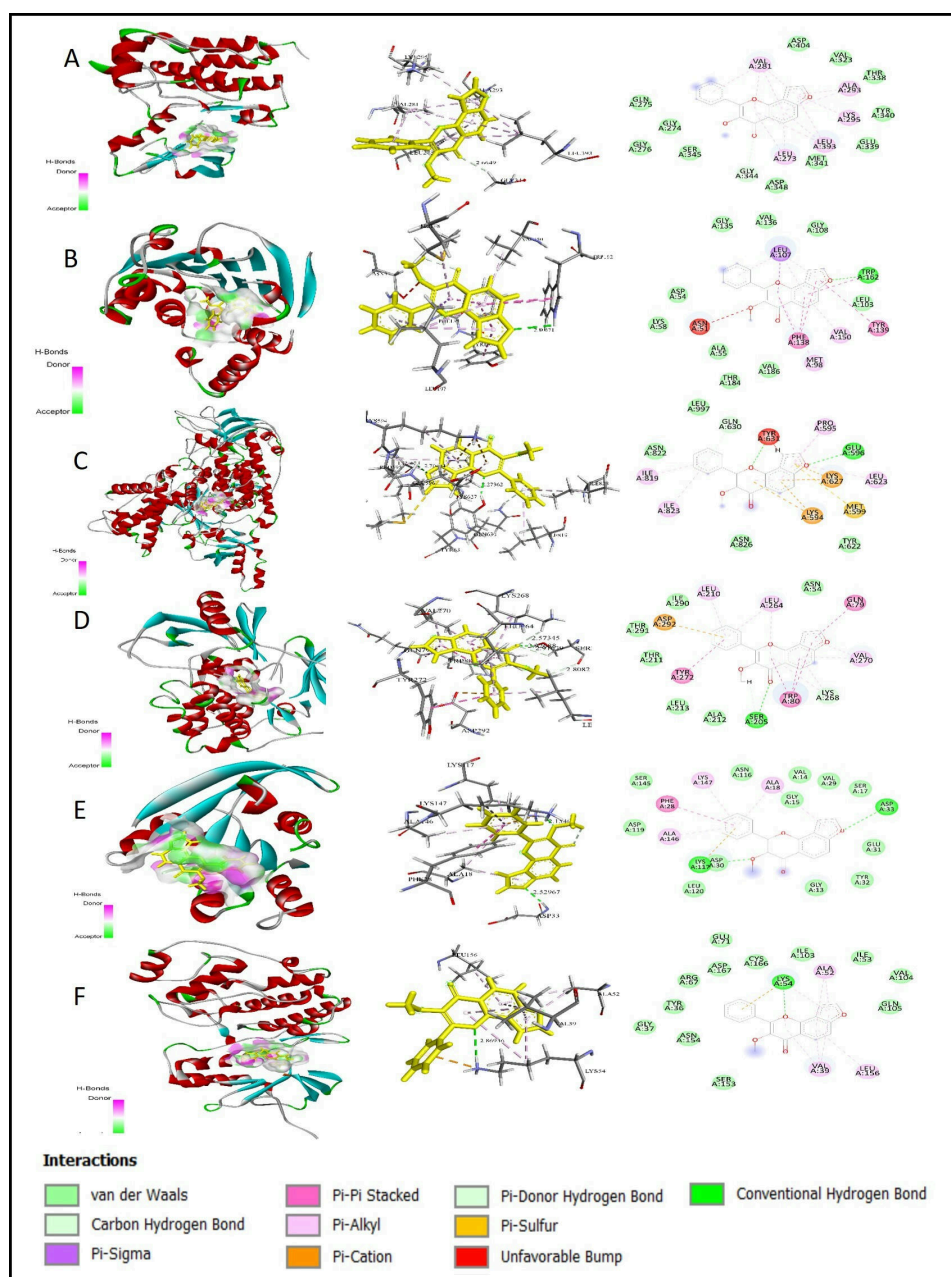

Figure 6. 3-D and 2-D diagrammatic representations of the molecular docking patterns between karanjin and various receptor proteins, generated using Discovery Studio (A) Karanjin-SRC (2bdf); (B) Karanjin-HSP90AA1 (4nh8); (C) Karanjin-PIK3CA (2rd0); (D) Karanjin-AKT1 (3o96); (E) Karanjin-HRAS (5p21); (F) Karanjin-MAPK1 (1tvo).
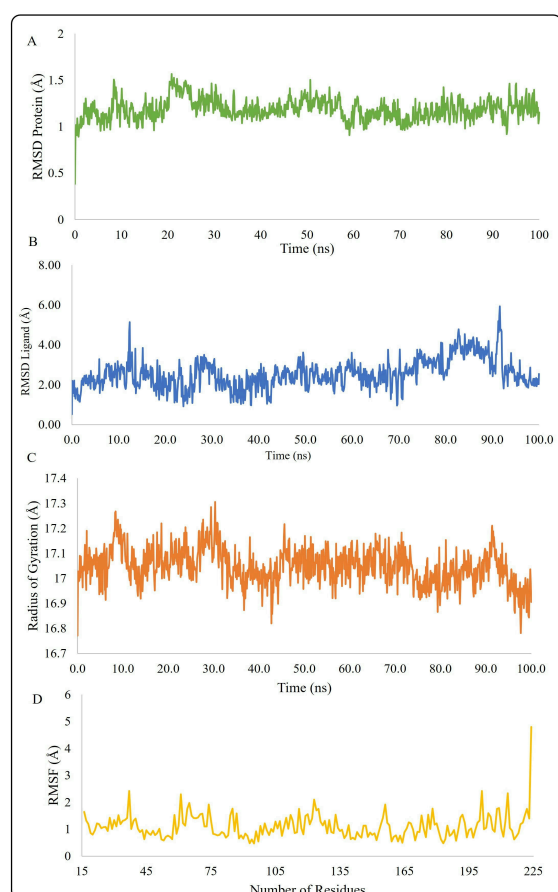
Figure 7. Molecular dynamics results of karanjin-HSP90AA1 complex (A) The RMSD of the docked protein (Å) versus MD simulation time (ns) determines the stability of the protein structure; (B) RMSD of the docked ligand (Å) versus MD simulation time (ns) determines the stability of the ligand; (C) Rg (Å) versus MD simulation time (ns) plot determines the flexibility of different regions of the protein.; (D) RMSF (Å) versus number of residues determines the overall compactness of the protein during the simulation.

This shows that both complexes are stable with very minor differences in their Rg values over the 100-ns simulation period.

According to the RMSF analysis of the karanjin-HSP90AA1 complex (Figure 7D), the highest RMSF peak was observed at 4.8 Å with the residue LYS224. All other residues showed lower fluctuations and were stable. In the karanjin-AKT1 complex (Figure 8D), the highest RMSF peak was observed at 4.65 Å of the residue GLN445. In addition to GLN445, ARG446 also showed a high peak at 3.69 Å. Hence, these two residues are responsible for the increased fluctuations. All other residues were found to be stable with fewer fluctuations.

DISCUSSION

A comprehensive assessment of ADME is essential in the initial stages of pharmaceutical drug discovery. This is a critical step in modern drug discovery. Early evaluation of these qualities

leads to the elimination of compounds with undesirable pharmacokinetic ADME properties, which is important for successful drug discovery.[22] The pharmacokinetic characteristics of karanjin were evaluated to determine its safety, efficacy, and toxicity. According to the findings (Table 1), karanjin did not violate any of Lipinski's rule of five. It has been noted that orally active drug compounds can violate up to two of Lipinski's rules.[23] This indicates the potential of karanjin as a drug-like molecule. Previous studies have reported that karanjin can be used as an active drug.[24] Identifying targets, particularly for polygenic diseases, is essential for drug development. The core phase involves recognising and validating drug targets of interest for downstream processes.[25]
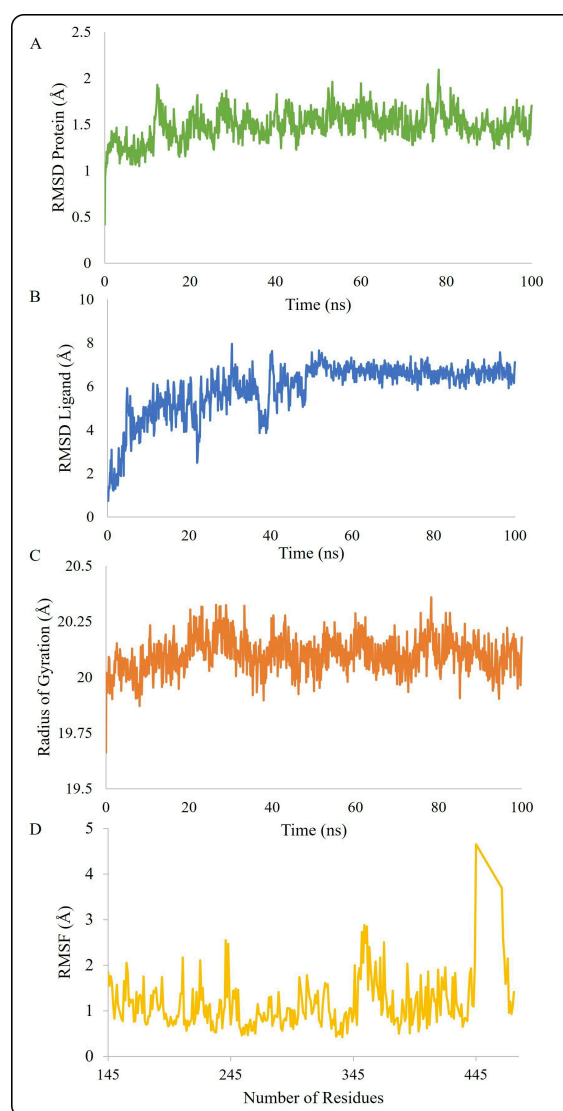

Figure 8. Molecular dynamics results of karanjin-AKT1 complex (A) The RMSD of the docked protein (Å) versus MD simulation time (ns) determines stability of protein structure; (B) RMSD of the docked ligand (Å) versus MD simulation time (ns) determines stability of ligand; (C) Rg (Å) versus MD simulation time (ns) plot determines the flexibility of different regions of the protein.; (D) RMSF (Å) versus number of residues determines the overall compactness of the protein during the simulation.

A total of 263 candidate genes for the karanjin effect on colorectal cancer were identified using a Venn diagram. A PPI network of 176 nodes and 542 edges revealed two clusters, and 24 key targets with AKT1, MAPK1, and SRC identified as the top three.

The GO project creates ontologies to describe gene product properties across three distinct domains of molecular biology.[26] The top terms include signal transduction, protein binding, and the cytosol. Karanjin targets the nucleoplasm, cytoplasm, and nucleus, with functions like ATP binding and kinase activity, impacting cell proliferation, apoptosis, migration, and MAPK cascade pathways. Therefore, karanjin may exert its anticancer properties via the aforementioned biological processes. Moreover, KEGG enrichment analysis revealed 20 significant pathways (p<0.01), with pathways in cancer and PI3K-Akt being the most enriched. An *in vitro* study by Roy et al. in 2021 elucidated that karanjin downregulated Cluster of differentiation 44 (CD44) signalling pathway in cervical cancer cell line.[11] CD44 is a transmembrane glycoprotein that is involved in various functions like cell proliferation, migration, adhesion by controlling cellular signalling pathway i.e., AKT1, MAPK1, mTOR, JNK etc.[11,27,28] A study conducted by Jinsong Yu and co-workers in 2022 showed that karanjin exhibited antitumor activity in breast cancer cells by regulating the PI3K/Akt signalling pathway.[29] KEGG enrichment analysis demonstrated the therapeutic role of karanjin in colon cancer via its effects on various signalling pathways.

Furthermore, in current drug development, molecular docking is an advanced computational technique that uses docking software to examine ligand-receptor interactions and assesses conformational and electrostatic interactions.[9] The results indicated that karanjin binds more efficiently to AKT1 (Figure 6D), potentially inhibiting it more effectively than other key targets, while the binding energy difference between the positive control and karanjin was greatest for the C-H-Ras p21 protein among all screened targets. RAS is a frequently mutated oncogene in human cancer, leading to common dysregulation of its pathway, while HRAS functions as a binary switch that shifts between an inactive GDP-bound state and an active GTP-bound state. In an active form, RAS stimulates various downstream signalling pathways, i.e., Raf-MEK-ERK pathway[30] and the phosphoinositide 3-kinase (PI3Ks) pathway.[31] The Ras/Raf/MAPK pathway is involved in cell cycle regulation, migration, and angiogenesis.[32] Karanjin binds with a docking score of 9.14 kcal/mol in the same binding region as that of GTP on HRAS on amino acid residues LYS117 and ASP33 (The Uniprot Consortium 2023) (https://www.uniprot.org/) (Figure 6E). Thus, GTPase HRAS may be a potential target of karanjin's anticancer potential.

Additionally, Heat shock protein 90-alpha (HSP90AA1) is a crucial molecular chaperone that has been conserved throughout evolution. Previous studies have shown that HSP90AA1 activates several oncogenic proteins in cancer cells, promoting cell survival, proliferation, and invasiveness.[33] Its expression is elevated in various cancers and is directly related to therapeutic resistance.[34] Moreover, HSP90AA1 may serve as a potential target for colorectal cancer treatment, as studies have indicated that it can promote cancer cell proliferation, metastasis, invasion, and epithelial-to-mesenchymal transition.[35] The ATP-binding site of HSP90AA1 comprises amino acid residues ASN51 and PHE138 (The UniProt Consortium 2023) (https://www.uniprot.org/). In several previous studies, binding with HSP90AA1at the residues ASN51 and PHE138 showed inhibition of its activity.[36-38] Hence, binding of karanjin with HSP90AA1 at amino acid residues ASN51 and PHE138 (Figure 6B) may prevent the binding of ATP and inhibit its activity.

In addition to AKT1, HSP90AA1 and HRAS are another efficiently interacting signalling pathways of mitogen-activated protein kinase (MAPK) that respond via a series of phosphorylation activities by transforming extracellular signals into cellular responses. Hence, deregulation of these pathways leads to cell proliferation, epithelial-to-mesenchymal transition (EMT), migration, or invasion. In colorectal cancer, RAS/BARF mutation leads to constitutive activation of ERK1/2 signalling cascade.[39] This suggests that MAPK inhibition represents a potential treatment for colorectal cancer. Karanjin binds to the ATP-binding pocket of MAPK1 protein (Figure 6F) by forming hydrogen bonds with amino acid residue LYS54 and by forming pi alkyl bonds with residues bond with amino acid residue LYS54 and by forming pi alkyl bond with residue ALA52, VAL39, and LEU156. The ATP-binding site of MAPK1 comprises amino acid residues 31-39 and 54 (The UniProt Consortium 2023). According to previous research, the selective and ATP-competitive well-known inhibitor FR180204 binds to MAPK1 in the same binding pocket and inhibits its activity via ATP binding.[40] These findings imply that karanjin can act as a MAPK-selective inhibitor, which is potentially valuable for drug development.

Molecular docking effectively predicts binding modes, but it struggles with accurate binding energy calculations because of approximations in solvent treatment, macromolecular flexibility and accurate modelling of metallic interactions.[41] Other factors such as receptor flexibility, multiple binding pockets, and polar interactions hinder correct pose prediction, limiting its wider application.[42] To overcome the shortcomings of molecular docking, molecular dynamics simulations can be used to enhance drug discovery by

optimising protein structures, refining docked complexes, and including solvent effects.[43] In line with the above findings, various dynamic parameters, including RMSD of the protein, RMSD of the ligand, RMSF, and Rg were analysed. RMSD and RMSF are the two most used metrics of structural fluctuations. RMSD is the average displacement of the atoms at a given instant in the simulation compared to a reference structure, which is often the simulation's first frame or the crystallographic structure. The RMSF is a measure of specific atoms or groups of atom displacement relative to the reference structure, averaged over the number of atoms.[44] Rg is an indicator of protein structural compactness and 3D structural stability. If a protein folds stably, its Rg value will most likely remain relatively constant. When a protein unfolds, its Rg changes over time.[45] Both the karanjin-HSP90AA1 and karanjin-AKT1 complexes exhibited stability with minimal fluctuations in their Rg values over the 100-ns simulation period. The stability of the karanjin-HSP90AA1 and karanjin-AKT1 complexes through molecular dynamics simulations were assessed in this research (Figure 7 and Figure 8). Upon evaluating various dynamic parameters, including the RMSD of the protein and ligand, the RMSF and Rg of both complexes demonstrated consistent stability throughout a 100-ns simulation period.

CONCLUSION

In conclusion, our study combined network pharmacology and molecular docking to provide a comprehensive understanding of the mechanisms through which karanjin may be effective in treating colorectal cancer. Karanjin is vital for colorectal cancer treatment, targeting multiple pathways and proteins. It exhibits anti-cancer effects by binding to AKT1, HSP90AA1, HRAS, and MAPK1, and may disrupt tumour cell proliferation and apoptosis by modulating the PI3K-Akt and MAPK signalling pathways, among others. MD simulations further supported the stable docked structure of karanjin with HSP90AA1 and AKT1. According to this *in silico* study, karanjin can be considered to be of great interest in successful chemotherapy, which opens a new avenue for *in vitro* and *in vivo* experiments to inhibit colorectal cancer using karanjin as an anticancer molecule.

Author Details

Khairah Ansari
[1] Gujarat University, Biomedical Technology and Human Genetics University School of Sciences, Department of Zoology, Ahmedabad, Gujarat, India
0000-0003-0634-0383

Priyesh Kumar
[1] Gujarat University, Biomedical Technology and Human Genetics University School of Sciences, Department of Zoology, Ahmedabad, Gujarat, India
0000-0002-4252-6882

Devendrasinh Jhala
[1] Gujarat University, Biomedical Technology and Human Genetics University School of Sciences, Department of Zoology, Ahmedabad, Gujarat, India
0000-0002-1339-6492   ddjhala@gmail.com

REFERENCES

1 Cooper GM, Hausman RE. The development and causes of cancer. In: The Cell: A Molecular Approach. 2nd ed. Sunderland, MA: Sinauer Associates; 2000:725-766.

2 Siegel RL, Wagle NS, Cercek A, Smith RA, Jernal A. Colorectal cancer statistics, CA. *Cancer J Clin.* 2023;73(3):233–254.

3 Vogelstein B, Kinzler KW. Cancer genes and the pathways they control. *Nat Med.* 2004;10(8):789–799.

4 Muhammad N, Usmani D, Tarique M, et al. The role of natural products and their multitargeted approach to treat solid cancer. *Cells* 2022;11(14):2209. doi:10.3390/cells11142209

5 Aschele C, Debernardis D, Bandelloni R, et al. Thymidylate synthase protein expression in colorectalcancer metastases predicts for clinical outcome to leucovorin-modulated bolus or infusional 5-fluorouracil but not methotreaxate modulate bolus 5-fluorouracil. *Ann Oncol.* 2002;12(13):1882-1892.

6 Hasima N, Aggarwal BB. Cancer-linked targets modulated by curcumin. *Int J Biochem Mol Bio.* 2012;3(4):328-351.

7 Song X, Zhang Y, Dai E, Wang L, Du H. Prediction of triptolide targets in rheumatoid arthritis using network pharmacology and molecular docking. *Int Immunopharmacol.* 2020;80:106179. doi.:10.1016/j.intimp.2019.106179

8 Dong Y, Zhao Q, Wang Y. Network pharmacology-based investigation of potential targets of astragalus membranaceous-angelica sinensis compound acting on diabetic nephropathy. *Sci Rep.* 2021;11(1):19496. doi:10.1038/s41598-021-98925-6

9 Pinzi L, Rastelli G. Molecular docking: Shifting paradigms in drug discovery. *Int J Mol Sci.* 2019;20(18):4331. doi:10.3390/ijms2018433

10 Guo JR, Chen QQ, Wai Kei Lam C, Zhang W. Effects of karanjin on cell cycle arrest and apoptosis in human A549, HepG2 and HL 60 cancer cells. *Biol Res.* 2015;48:1-7. doi:10.1186/S40659-015-0031-X

11 Roy R, Mandal S, Chakrabarti J, Saha P, Panda CK. Downregulation of hyaluronic acid-CD44 signaling pathway in cervical cancer cell by natural polyphenols plumbagin, pongapin and karanjin. *Mol Cell Biochem.* 2021;476(10):3701–3709.

12 Zhang J, Xie Y, Fan Q, Wang C. Effects of karanjin on dimethylhydrazine induced colon carcinoma and aberrant crypt foci are facilitated by alteration of the p53/Bcl2/BAX pathway for apoptosis. *Biotech Histochem.* 2021;96(3):202-212.

13 Lipinski CA, Discovery M, Lombardo F, et al. Experimental and computational approaches to estimate solubility and permeability in drug discovery and development settings. *Adv Drug Deliv Rev.* 1997;23(1-3):3–25.

14 Gfeller D, Grosdidier A, Wirth M, et al. SwissTargetPrediction: A web server for target prediction of bioactive small molecules. *Nucleic Acids Res.* 2014;42(W1):W32-W38.

15 Gaulton A, Bellis LJ, Bento AP, et al. ChEMBL:A large-scale bioactivity database for drug discovery. *Nucleic Acids Res.* 2012;40(D1):D1100-D1107.

16 Saito R, Smoot ME, Ono K, et al. A travel guide to cytoscape plugins. *Nat Methods.* 2012;9(11):1069–1076.

17 Dennis G, Sherman BT, Hosack DA, et al. DAVID: Database for annotation, visualization, and integrated discovery. *Genome Biol.* 2003;4(5):1-11. doi:10.1186/GB-2003-4-9-R60.

18 Kanehisa M, Furumichi M, Tanabe M, Sato Y, Morishima K. KEGG: New perspectives on genomes, pathways, diseases and drugs. *Nucleic Acids Res.* 2017;45(D1):D353–D361.

19 Tian W, Chen C, Lei X, Zhao J, Liang J. CASTp 3.0: Computed atlas of surface topography of proteins. *Nucleic Acids Res.* 2018;46(W1):W363-W367.

20 Krieger E, Vriend G. YASARA View—molecular graphics for all devices—from smartphones to workstations. *Bioinformatics.* 2014;30(20):2981–2982.

21 Liu X, Ouyang S, Yu B, et al. PharmMapper server: A web server for potential drug target identification using pharmacophore mapping approach. *Nucleic Acids Res.* 2010;38:W609-W614.

22 Vrbanac, J., Slauter, R. ADME in Drug Discovery. In:A Comprehensive Guide to Toxicology in Nonclinical Drug Development Elsevier: Amsterdam, The Netherlands, 2017;39–67. doi:10.1016/B978-0-12-803620-4.00003-7

23 Benet LZ, Hosey CM, Ursu O, Oprea TI. BDDCS, the Rule of 5 and drugability. *Adv Drug Deliv Rev.* 2016;101:89–98.

24 Das S, Tiwari GJ, Ghosh A. In silico analysis of new flavonoids from *Pongamia pinnata* with a therapeutic potential for age-related macular degeneration. *3 Biotech.* 2020;10(12):1–6. doi:10.1007/s13205-020-02537-2

25 Agamah FE, Mazandu GK, Hassan R, et al. Computational/in silico methods in drug target and lead prediction. *Brief Bioinform.* 2020;21(5):1663–1675.

26 Ashburner M, Ball CA, Blake JA, et al. Gene Ontology: Tool for the unification of biology. *Nat Genet.* 2000;25(1):25-29.

27 Chen C, Zhao S, Karnad A, Freeman JW. The biology and role of CD44 in cancer progression: therapeutic implications. *J Hematol Oncol.* 2018;11(1):1–23. doi:10.1186/S13045-018-0605-5

28 Wang L, Zuo X, Xie K, Wei D. The role of CD44 and cancer stem cells. *Methods Mol Bio.* 2018;1692:31–42.

29 Yu J, Yang H, Lv C, Dai X. The cytotoxicity of karanjin toward breast cancer cells is involved in the PI3K/Akt signaling pathway. *Drug Dev Res.* 2022;83(7):1673–1682.

30 Moodie SA, Willumsen BM, Weber MJ, Wolfman A. Complexes of Ras·GTP with Raf-1 and mitogen-activated protein kinase kinase. *Science.* 1993;260(5114):1658–1661.

31 Castellano E, Downward J. RAS interaction with PI3K: More than just another effector pathway. *Genes Cancer.* 2011;2(3):261–274.

32 Molina JR, Adjei AA. The Ras/Raf/MAPK pathway. *J Thorac Oncol.* 2006;1(1):6-7. doi:10.1016/s1556-0864(15)31506-9

33 Liu H, Zhang Z, Huang Y, et al. Plasma HSP90AA1 predicts the risk of breast cancer onset and distant metastasis. *Front Cell Dev Biol.* 2021;9:639596. doi:10.3389/fcell.2021.639596

34 Calderwood SK, Khaleque MA, Sawyer DB, Ciocca DR. Heat shock proteins in cancer: Chaperones of tumorigenesis. *Trends Biochem Sci.* 2006;31(3):164–172.

35 Zhang M, Peng Y, Yang Z, et al. DAB2IP down-regulates HSP90AA1 to inhibit the malignant biological behaviors of colorectal cancer. *BMC Cancer.* 2022;22(1):1-15. doi:10.1186/s12885-022-09596-z

36 Moon SJ, Jeong BC, Kim HJ, et al. Bruceantin targets HSP90 to overcome resistance to hormone therapy in castration-resistant prostate cancer. *Theranostics.* 2021;11(2):958-973.

37 Sain A, Khamrai D, Kandasamy T, Naskar D. Apigenin exerts anti-cancer effects in colon cancer by targeting HSP90AA1. *Biomol Struct Dyn.* 2023;1-13. doi:10.1080/07391102.2023.2299305

38 Zhou Y, Wu C, Qian X, et al. Multitarget and multipathway regulation of zhenqi fuzheng granule against non-small cell lung cancer based on network pharmacology and molecular. *Evid Based Complement Alternat Med.* 2022;2022(5967078):1-16. doi:10.1155/2022/5967078.

39 Urosevic J, Nebreda AR, Gomis RR. MAPK signaling control of colon cancer metastasis. *Cell Cycle.* 2014;13(17):2641–2642.

40 Ohori M, Kinoshita T, Okubo M, et al. Identification of a selective ERK inhibitor and structural determination of the inhibitor–ERK2 complex. *Biochem Biophy Res Commun.* 2005;336(1):357–363.

41 Prieto-Martínez FD, Arciniega M, Medina-Franco JL. Molecular docking: Current advances and challenges. *Tip Rev Espec Cienc Quím-Biol.* 2018;21(1):1-23. doi:10.22201/fesz.23958723e.2018.0.143

42 Kolb P, Irwin JJ. Docking screens: right for the right reasons? *Curr top Med Chem.* 2009;9(9):755-770.

43 Alonso H, Bliznyuk AA, Gready, JE. Combining docking and molecular dynamic simulations in drug design. *Med Res Rev.* 2006;26(5):531-568.

44 Martínez, L. Automatic identification of mobile and rigid substructures in molecular dynamics simulations and fractional structural fluctuation analysis. *PLoS One.* 2015;10(3):e0119264. doi:10.1371/journal.pone.0119264

45 Sneha P, Priya DCG. Molecular dynamics: New frontier in personalized medicine. *Adv Protein Chem Struct Biol.* 2016;102:181–224.